Penerbit Akademia Baru

Journal of Advanced Research in Fluid Mechanics and Thermal Sciences

Journal homepage: www.akademiabaru.com/arfmts.html
ISSN: 2289-7879

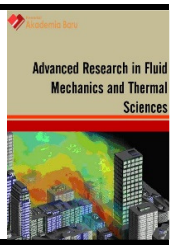

CFD Simulation of Temperature and Air Flow Distribution inside Industrial Scale Solar Dryer

Open Access

Arina Mohd Noh[1,2,*], Sohif Mat[1], Mohd Hafidz Ruslan[1]

[1] Solar Energy Research Institute (SERI), Universiti Kebangsaan Malaysia, 43600 Bangi, Selangor, Malaysia
[2] Engineering Research Center, Ibu Pejabat MARDI, 43400 Serdang, Selangor, Malaysia

ARTICLE INFO

Article history:
Received 1 March 2018
Received in revised form 23 April 2018
Accepted 12 May 2018
Available online 17 May 2018

ABSTRACT

Drying is an important process in many industries to reduce moisture content inside the product to a safe limit to reduce losses or as a requirement for the downstream processes. It's also contribute in reducing the handling and storage cost. In convective drying, temperature and velocity of the drying air have been identified as the important factors that effecting the drying rate of the product. New solar drying have been developed for sericite mica drying process. The objectives of this paper are to simulate and analyze the effect of product arrangement and different operating condition on the temperature and airflow distribution inside the drying chamber of the newly developed solar dryer. Commercial CFD software, Ansys Fluent was used in the study. The results from CFD simulations shows that the zig zag pallet arrangement produces higher and more uniform air flow compared to the straight pallet arrangement. Three possible operating conditions for the solar dryer have been identified and simulated which are greenhouse effect with passive ventilation, greenhouse effect with active ventilation and greenhouse effect with intermittent active ventilation. CFD simulation results show that the operating condition with intermittent active ventilation produce the highest temperature for both inside the drying chamber and inside the sericite mica which is up to 59.8 and 55.6^{o}C respectively.

Keywords:
Solar dryer, CFD simulation, air flow distribution, temperature distribution

1. Introduction

Drying is a process to remove moisture from a product to a certain safe limit. Drying processes consume large amounts of energy and any improvement in existing dryer design that leads to cost reductions and product quality improvements will definitely beneficial for the industry. Development of the solar dryer was beneficial to the drying process due to the fact that it's used solar energy as a main energy source which is free and cause no negative impact to the environment. Previous research has proven that compare to open sun drying, solar dryers show faster drying rates by achieving higher temperatures, lower humidity, and increased air movement in the drying chamber. Solar dryer also has proven able to improve product quality in terms of flavor, color, and appearance.

* *Corresponding author.*
E-mail address: arinamn@gmail.com (Arina Mohd Noh)

In the drying process, drying air temperature and velocity are the main factors that affects the drying rate of the product. The study by Raka Noveriyan Putra and Tri Ayodha Ajiwiguna [1] proved that the increasing of drying air temperature and velocity causes higher evaporation rate. Study by Matuam Balbine *et al.*, [2] also concluded that higher air temperature led to the faster drying rate and shorter drying time. The study also found that the quality of the final dried product also depends on the uniformity of the drying air distribution.

In designing suitable geometric configurations of the drying chamber, the prediction of the airflow and temperature inside the dryer helps to optimize the design and improving the drying process before the actual dryer was built. Numerical techniques have been used to numerically model the behavior of the airflow inside several kinds of dryers [3-5]. However, this process is tedious and involve a complex mathematical formulation. Computational fluid dynamics (CFD) is a widely accepted technique and tool for numerical simulations of such systems. CFD has been proven as an effective computational tool for predicting the flow behavior and mass transfer phenomena occurring in multicomponent systems in many industries [6-7]. Mujumdar and Wu [8] have emphasized that the CFD approach is the cost-effective solutions that can push innovation and creativity in drying equipment design and development. During the drying process, especially for large scale dryer, measurement of air velocities and temperature is tedious and difficult, since several sensors are needed to be placed at various locations and directions of air flow, therefore CFD software may be used to predict the air velocities and temperature in the drying chamber. The simulation results from CFD need to be compared with actual drying experiments and if there is an agreement between predicted and experimental results, then the CFD code may be applied for other drying conditions to optimize the drying performance of the dryer. This have been proved by study of many researchers [9-15] and shows that the performance of new dryer designs can be predicted by CFD simulation work. These studies also proved that the CFD simulation result is comparable with actual conditions.

In this study, an industrial scale solar dryer was developed to dry sericite mica. Sericite mica is an inorganic mineral belongs to mica group. In the production of sericite mica drying is important as it is the requirement of the downstream processes and also to reduce the handling cost and ease the handling process. The developed solar dryer was a greenhouse type solar dryer equipped with a blower for active ventilation during the drying process. Although active ventilation is more efficient and shows higher drying rate compare to passive ventilation [16], it requires higher energy cost. This study will analyze the possibility of using intermittent ventilation instead of continuous passive or active ventilation to reduce the cost of the drying process. The analysis will focus on the airflow and temperature distribution inside the drying chamber with different product arrangement and different operating condition. The Intermittent drying technique has been studied by many researchers and its shows significant improvement not only in energy savings but also the quality of the dried product [17].

2. Methodology

The developed industrial scale solar dryer consists of evacuated tubes, heat exchanger, blower and drying chamber. The drying chamber size was 1.25m height x 1.7m width x 17m long. The drying chamber was made of polycarbonate sheet. The heat exchanger and blower was placed at one end of the drying chamber where we call it the inlet. The evaporated moisture from the sericite mica is removed to the environment through the opening at the other end of the drying chamber which is the outlet. The evacuated tube will absorb heat from the sun and heated the water that are flowing

in the piping system. At the inlet the heat exchanger will transfer the heat from the water into the air and the blower will produce an air flow with a speed of 3ms^{-1} into the drying chamber.

The drying chamber can accommodate up to 10 pallets per batch of drying. In the current practice of solar drying, about 60 pieces of sericite mica were stacked up on the pallet in 4 rows as shown in figure 1(a). However this method caused the slow drying rate and sometimes it takes up to 3 months to dry the whole sericite mica. In the new solar dryer different arrangement of sericite mica was applied. 8 pieces of sericite mica were placed on each pallet and 5 pallets were stacked up on top of each other as shown in figure 1(b).

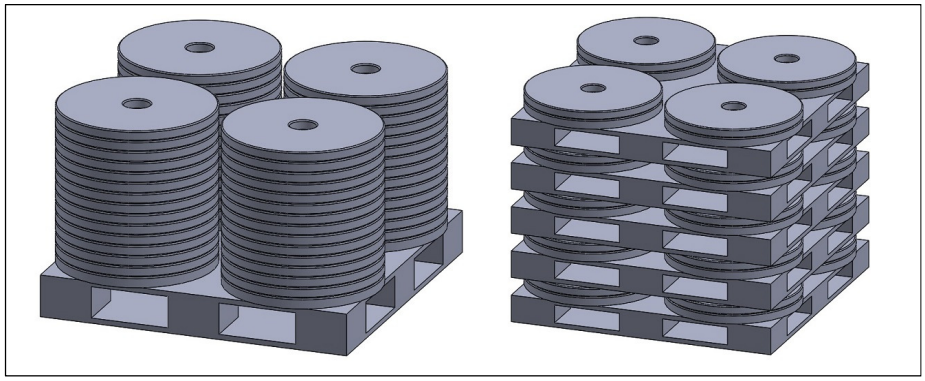

(a) (b)

Fig. 1. Arrangement of sericite mica on the pallet (a) current and (b) new

In this study commercial CFD software ANSYS ver.14 was used to simulate air flow and temperature distribution in the drying chamber. Ansys Fluent used numerical finite volume methods to solve the equation. The governing equations of fluid flow and heat transfer was considered as mathematical formulations of the conservation laws of fluid mechanics and are referred to as the Navier-Stokes equations [18]. By enforcing these conservation laws over discrete spatial volumes in a fluid domain, it is possible to achieve a systematic account of the changes in mass, momentum and energy as the flow crosses the volume boundaries. In Ansys fluent the resulting equations were written as below [19]:

Continuity equation:

$$\frac{\partial \rho}{\partial t} + \nabla.(\rho \vec{v}) = S_M \quad (1)$$

Momentum equation:

$$\frac{\partial}{\partial t}(\rho \vec{v}) + \nabla.(\rho \vec{v}\vec{v}) = -\nabla p + \nabla.(\bar{\bar{\tau}}) + \rho \vec{g} + \vec{F} \quad (2)$$

Energy equation:

$$\frac{\partial}{\partial t}(\rho E) + \nabla.\left(\vec{v}(\rho E + p)\right) = \nabla.\left[k_{eff}\nabla T - \sum_j h_j \vec{J}_j + (\bar{\bar{\tau}}_{eff}.\overrightarrow{v})\right] + S_h \quad (3)$$

The first three terms on the right-hand side of Equation (3) represent an energy transfer due to conduction, species diffusion, and viscous dissipation, respectively.

The turbulent kinetic energy, k, and its rate of dissipation, ε, are obtained from the following transport equations:

$$\frac{\partial}{\partial t}(\rho k) + \frac{\partial}{\partial x}(\rho k u_i) = \frac{\partial}{\partial x_j}\left[\left(\mu + \frac{\mu_t}{\sigma_k}\right)\frac{\partial k}{\partial x_j}\right] G_k + G_b - \rho\varepsilon - \gamma_M - S_k \quad (4)$$

$$\frac{\partial}{\partial t}(\rho \varepsilon) + \frac{\partial}{\partial x}(\rho \varepsilon u_i) = \frac{\partial}{\partial x_j}\left[\left(\mu + \frac{\mu_t}{\sigma_\varepsilon}\right)\frac{\partial \varepsilon}{\partial x_j}\right] + C_{1\varepsilon}\frac{\varepsilon}{k}(G_k + C_{3\varepsilon}G_b) - C_{2\varepsilon}\rho\frac{\varepsilon^2}{k} + S_\varepsilon \quad (5)$$

In this study a solar load model was used to calculate radiation effects from the sun's rays that enter a computational domain. The fair weather condition option was selected because this method imposes greater attenuation on the solar load which is representative of atmospheric conditions that are fair but not completely clear. The equation for normal direct irradiation applying the Fair Weather Conditions Method is taken from the ASHRAE Handbook [19]:

$$Edn = \frac{A}{e^{\frac{B}{\sin\beta}}} \quad (6)$$

where A is solar irradiation at air mass = 0 (Wm^{-2}), B is Atmospheric extinction coefficient and β is Solar altitude (in degrees) above the horizontal.

To save the computational time the CFD simulation only carried out for half of the dryer which consist only 5 stacks of pallet. Unstructured 3D tetrahedral mesh was used to mesh the solid geometry. The solar loading model was used in the simulation for the direct heat gain from the sun to the drying chamber. CFD simulation was used to analyze the airflow pattern between 2 types of product arrangement as shown in figure 2. In the new arrangement, instead of arranging the pallet in a straight line, the pallet arranged in zig zag pattern to allow the airflow in between the pallet. The setting of the product arrangement with better airflow will then be used in the analysis of different drying conditions that was possible for the newly developed solar dryer.

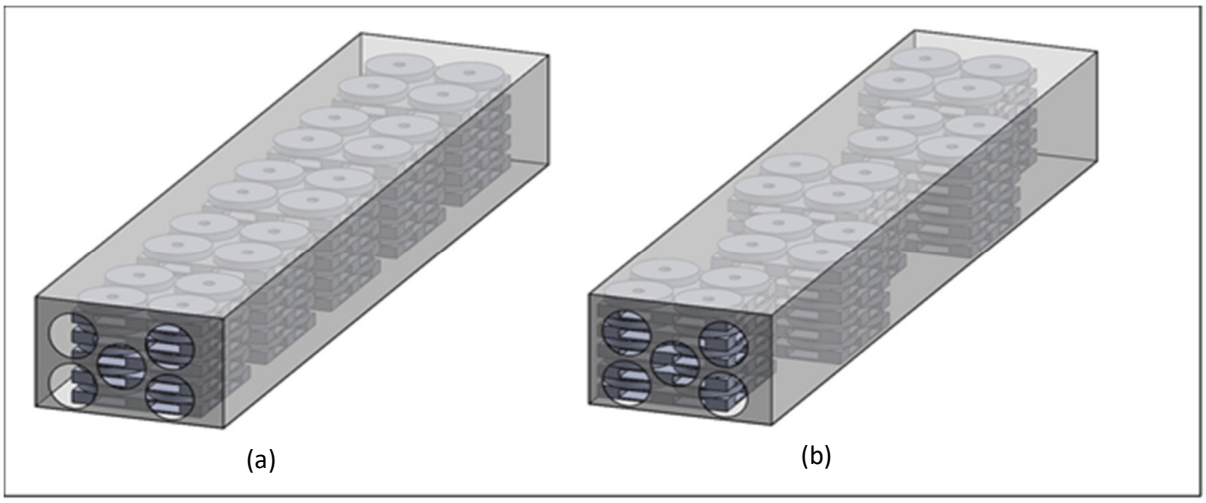

Fig. 2. Pallet arrangement inside the drying chamber (a) straight line (b) zig zag pattern

The newly developed solar dryer can be operated in three different conditions which are drying only using the greenhouse effect with passive ventilation, drying with greenhouse effect combine with continuous active ventilation and drying with greenhouse effect combine with intermittent active ventilation. Due to the size and capacity of the dryer, running a physical experiment is time consuming and involving many sensors and high labor cost. In this study CFD simulation was used to simulate these three possible modes of operations and to identify the most suitable mode of operation that will be carried out in the actual physical experiment. The simulation was carried out with different boundary condition according to the mode of operation as listed in the table 1 below.

Table 1
Summary of boundary condition for all conditions

Boundary condition	Condition 1 (greenhouse effect with passive ventilation)	Condition 2 (greenhouse effect combine with continuous active ventilation)	Condition 3 (greenhouse effect combine with intermittent active ventilation
Inlet velocity (ms^{-1})	Not available	3	3 (in active mode) 0 (in passive mode)
Inlet temperature (^oC)	Not available	50	60 (in active mode)
Time	Continuously for 20 minutes	Continuously for 20 minutes	Active mode for 10 minutes and passive mode for 10 minutes

The material properties used in the simulation are as shown in table 2 below:

Table 2
Material properties

Properties	Sericite mica	Pallet (wood)	Polycarbonate
Density (kg/m^3)	2820	700	1190
Thermal conductivity (W/m-k)	0.35	0.173	0.2
Specific heat (J/kg-k)	210	2310	1100

3. Results and Discussions

Figure 3 shows the result of air flow patterns inside the drying chamber with a straight and zig zag pallet arrangement. The figure shows that with the straight pallet arrangement the air flow was strong only at the side of the drying chamber while in between the pallet the air flow is low. This condition will cause un-uniform moisture removal from the product where the product located near the drying chamber wall will tend to remove the moisture faster compare to the one that are located in the middle. For the drying chamber with the zig zag arrangement, the figure shows that strong air flow was flowing in between each pallet. It shows that almost all products received the same amount of air flow and indirectly will cause more uniform moisture removal rate. From this result, zigzag arrangement was selected as the final arrangement and used in the simulation of different operating condition of the solar dryer.

Figure 4, 5, 6 and 7 shows the temperature distribution inside the drying chamber for condition 1, 2 and 3 respectively. The value of the temperature at three different locations which is at the inlet, centre and outlet of the drying chamber was measured to compare the results of the three conditions. The temperature at the centre of the sericite mica was also measured for comparison. Figure 8 shows the location of measured temperature. Figure 4 shows that for condition 1 where only the greenhouse effect takes place, the temperature inside the drying chamber increase up to 40.8^oC at point 3 and the temperature gradually decrease towards the outlet which is 38.5^oC at point

2 and 32.7°C at point 1. This is due to the opening at the outlet area. The temperature inside the sericite mica in this condition was increased up to 36.9°C.

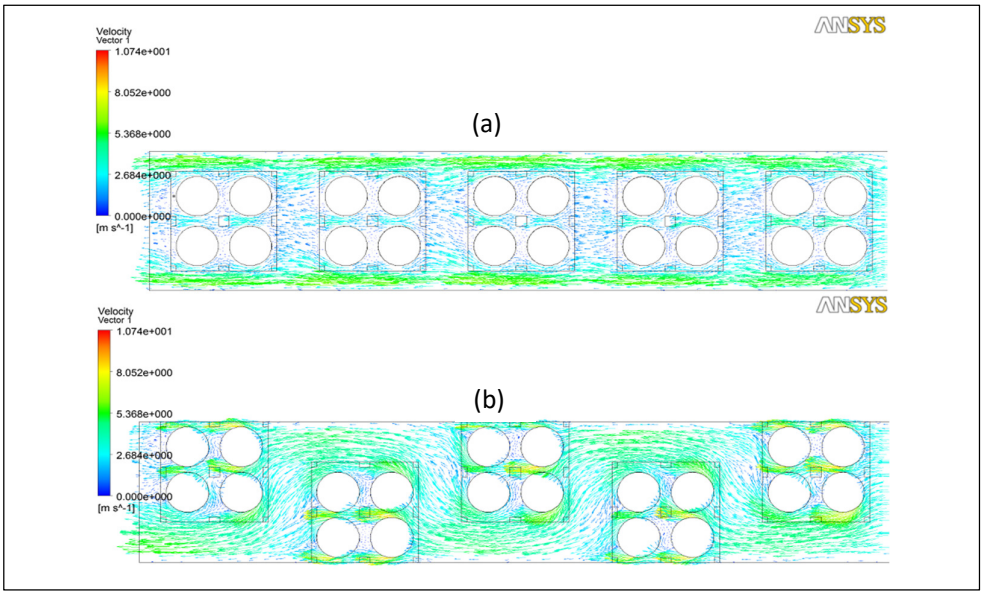

Fig. 3. Air flow pattern inside the drying chamber (a) straight pallet arrangement (b) zig zag pallet arrangement

In condition 2, as shown in figure 5 the temperature inside the drying chamber is uniformly distributed. The temperature was almost similar at point 1, 2 and 3 which are 44.7, 44.9 and 45°C respectively. The temperature inside the sericite mica for condition 2 was 45.7°C. The overall result for condition 2 was higher compare to condition 1 because the hot air from the solar system is streamed by the blower into the drying chamber.

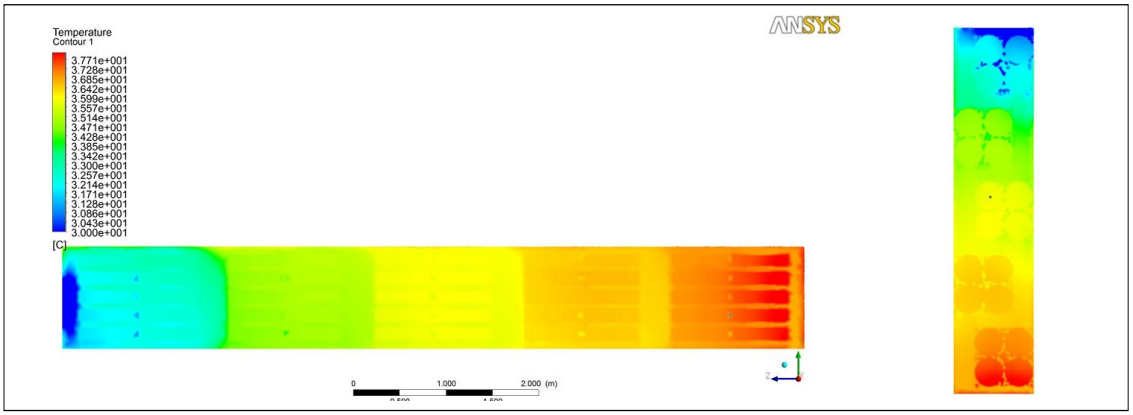

Side view Top view

Fig. 4. Temperature distribution inside the drying chamber for condition 1

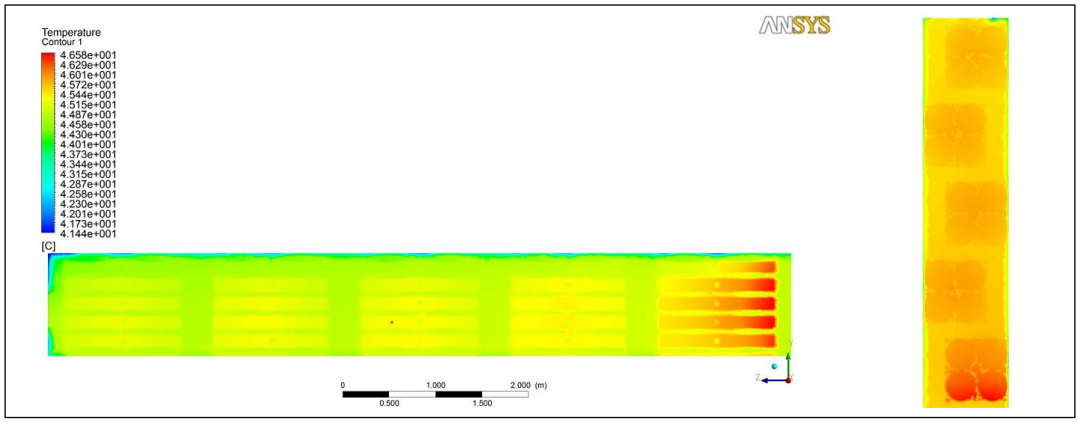

Side view Top view

Fig. 5. Temperature distribution inside the drying chamber for condition 2

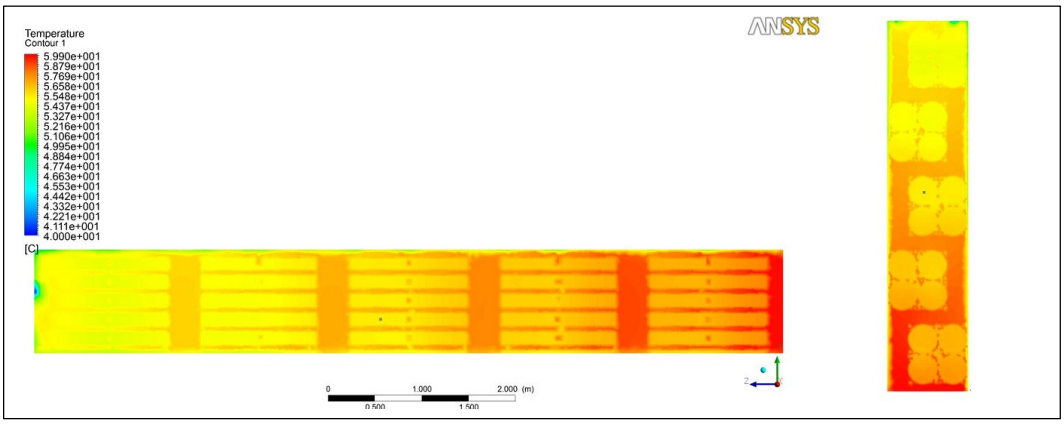

Side view Top view

Fig. 6. Temperature distribution inside the drying chamber for condition 3 (active mode)

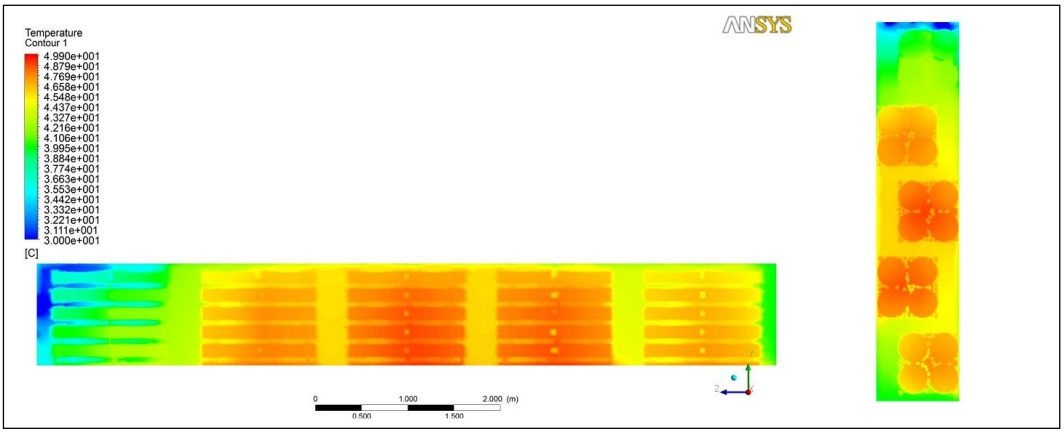

Side view Top view

Fig. 7. Temperature distribution inside the drying chamber for condition 3 (passive mode)

In condition 3, figure 6 shows the temperature distribution at the end of active mode and figure 7 shows the temperature distribution inside the drying chamber 10 minutes after the blower is off (passive mode). Temperature data inside the drying chamber in the active mode shows a temperature of 56, 57 and 59°C at point 1, 2 and 3 respectively while the temperature inside the sericite mica (point 4) was 55°C. After the blower turns off for 10 minutes, the temperature at point 1, 2 and 3 was reduced to 38, 46 and 47°C respectively. The temperature inside the sericite mica also reduce to 48°C. Table 3 summarizes the temperature at point 1, 2, 3 and 4 for all cases.

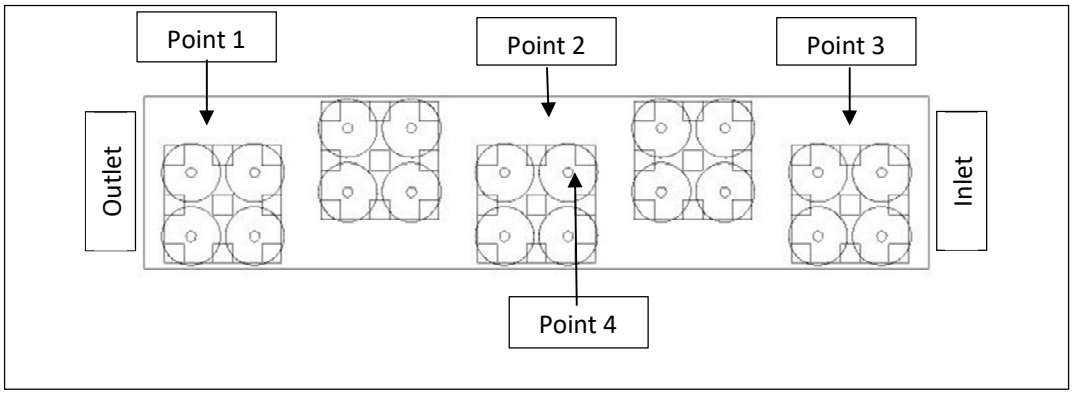

Fig. 8. Location of measurement point

Table 3
Summary of temperature data

Location	Condition 1 (°C)	Condition 2 (°C)	Condition 3 (active mode) (°C)	Condition 3 (passive mode) (°C)
Point 1	32.7	44.7	56.0	38.7
Point 2	38.5	44.9	57.6	46.2
Point 3	40.8	45.0	59.8	47.8
Point 4 (inside sericite mica)	36.9	45.7	55.6	48.5

From the result of temperature data, it shows that condition 3 produce the highest temperature inside the drying chamber and also inside the sericite mica compare to condition 1 and 2. However in terms of uniformity, condition 2 produces more uniformly distributed temperature compare to condition 1 and condition 3.

4. Conclusions

From the study it was concluded that CFD simulation was able to simulate and predict the temperature and air flow distribution inside the developed industrial scale solar dryer for various possible operating condition without the need to run the physical experiment which is time consuming, tedious and involve high cost. From the simulation results it shows that condition 3 is the most optimum condition that produce highest temperature inside the drying chamber and also inside the sericite mica. Although the temperature in the drying chamber is reduced in passive mode the temperature inside the sericite mica still higher compared to condition 1 and condition 2. Besides that, the major advantages of operating the solar dryer in condition 3 is the electrical energy savings

aspect as the blower only switch on intermittently compare to continuous mode where the blower is always turn on.

Acknowledgement
The authors would like to thank the Universiti Kebangsaan Malaysia (UKM) and Malaysia Agriculture Research and Development (MARDI) for sponsoring this work.

References

[1] Putra, Raka Noveriyan, and Tri Ayodha Ajiwiguna. "Influence of air temperature and velocity for drying process." *Procedia engineering* 170 (2017): 516-519.
[2] Balbine, Matuam, Edoun Marcel, Kuitche Alexis, and Zeghmati Belkacem. "Experimental Evaluation of the Thermal Performance of Dryer Airflow Configuration." *International Journal of Energy Engineering* 5, no. 4 (2015): 80-86.
[3] Ficarella, A., A. Perago, G. Starace, and D. Laforgia. "Thermo-fluid-dynamic investigation of a dryer, using numerical and experimental approach." *Journal of food engineering* 59, no. 4 (2003): 413-420.
[4] Mabrouk, Salah Ben, Besma Khiari, and Mohamed Sassi. "Modelling of heat and mass transfer in a tunnel dryer." *Applied thermal engineering* 26, no. 17-18 (2006): 2110-2118.
[5] Janjai, S., N. Srisittipokakun, and B. K. Bala. "Experimental and modelling performances of a roof-integrated solar drying system for drying herbs and spices." *Energy* 33, no. 1 (2008): 91-103.
[6] Zuan, A. M. S., S. S. Hidayah, S. Syahrullail, M. N. Musa, and E. A. Rahim. "Flow Analysis of Cooling Water in the Gas Turbine Fin Fan Cooler at Utilities Plant."
[7] Zhang, Jianping, Wayde Johnson, and Tom Plikas. "Application of computational fluid dynamics for solving ventilation problems in metallurgical industrial processes." *International Journal of Ventilation* 16, no. 3 (2017): 200-212.
[8] Mujumdar, Arun S., and Wu Zhonghua. "Thermal drying technologies—Cost-effective innovation aided by mathematical modeling approach." *Drying Technology* 26, no. 1 (2007): 145-153.
[9] Misha, Suhaimi, Sohif Mat, Mohd Hafidz Ruslan, Kamaruzzaman Sopian, and Elias Salleh. "The prediction of drying uniformity in tray dryer system using CFD simulation." *International Journal of Machine Learning and Computing* 3, no. 5 (2013): 419.
[10] Yunus, Y. M., and Hussain H. Al-Kayiem. "Simulation of hybrid solar dryer." In *IOP Conference Series: Earth and Environmental Science*, vol. 16, no. 1, p. 012143. IOP Publishing, 2013.
[11] Ranjbaran, Mohsen, Bagher Emadi, and Dariush Zare. "CFD simulation of deep-bed paddy drying process and performance." *Drying technology* 32, no. 8 (2014): 919-934.
[12] Romero, V. M., E. Cerezo, M. I. Garcia, and M. H. Sanchez. "Simulation and validation of vanilla drying process in an indirect solar dryer prototype using CFD Fluent program." *Energy Procedia* 57 (2014): 1651-1658.
[13] Somsila, Praphanpong, and Umphisak Teeboonma. "Investigation of temperature and air flow inside Para rubber greenhouse solar dryer incline roof type by using CFD technique." *Advanced Materials Research* (2014).
[14] Nazghelichi, Tayyeb, Arezou Jafari, Mohammad Hossein Kianmehr, and Mortaza Aghbashlo. "CFD simulation and optimization of factors affecting the performance of a fluidized bed dryer." *Iranian Journal of Chemistry and Chemical Engineering (IJCCE)* 32, no. 4 (2013): 81-92.
[15] Misha, S., Sohif Mat, Mohd Hafidz Ruslan, Kamaruzzaman Sopian, and E. Salleh. "Comparison between 2D and 3D simulations of a tray dryer system using CFD software." *World Applied Sciences Journal* 29, no. 10 (2014): 1301-1309.
[16] Patil, Rajendra, and Rupesh Gawande. "A review on solar tunnel greenhouse drying system." *Renewable and sustainable energy reviews* 56 (2016): 196-214.
[17] Franco, Rufino, and A. G. Barbosa de Lima. "Intermittent Drying of Porous Materials: A Review." In *Diffusion Foundations*, vol. 7, pp. 1-13. Trans Tech Publications, 2016.
[18] Norton, Tomás, and Da-Wen Sun. "Computational fluid dynamics (CFD)–an effective and efficient design and analysis tool for the food industry: a review." *Trends in Food Science & Technology* 17, no. 11 (2006): 600-620.
[19] ANSYS Fluent Theory Guide